# **Environment Protection Engineering**

Vol. 51 2025 No. 3

DOI: 10.37190/EPE/207494

GUANGHONG SHENG (ORCID: 0000-0003-1751-8044)<sup>1</sup>, WEIJIAN LIANG<sup>1</sup> SHIYU LUO<sup>1</sup>, SHISHENG WANG<sup>1</sup>, YIYUN LIU<sup>1</sup>, LEPING LIU<sup>1</sup>

# REMOVAL OF HIGH-CONCENTRATION FLUORIDE WASTEWATER BY CALCINED HYDRATED CALCIUM ALUMINATE WITH A TWO-STEP PROCESS

Hydrated calcium aluminate for fluoride removal of high-concentration fluoride-containing wastewater was prepared by thermal activation. X-ray fluorescence spectroscopy (XRF), X-ray diffraction (XRD), field emission scanning electron microscope (FE-SEM), The Fourier transform infrared spectrometry (FT-IR) were used to study the adsorption process. The results showed that the main component of the modified calcium aluminate cement (CAC) was 12CaO·7Al<sub>2</sub>O<sub>3</sub> (C<sub>12</sub>A<sub>7</sub>), and a large amount of calcium and aluminum ions were released during the fluoride removal process. The calcination of hydrated calcium aluminate improved the removal rate of fluoride. After a two-step treatment, adsorption and pH modification, the concentration of fluoride-containing solution from 300 mg/dm³ was reduced to less than 1 mg/dm³. Fluoride removal relies primarily on adsorption at low concentrations, whereas chemical precipitation dominates at high concentrations. The process involves three mechanisms: chemical precipitation, ion exchange, and electrostatic interaction.

## 1. INTRODUCTION

Fluoride-containing wastewater is discharged from many industries, such as metal smelting, aluminum electrolysis, rare earth separation, photovoltaic industry, lithium-ion batteries, etc., which is harmful to human health and the environment [1]. This type of wastewater can be discharged to a receiver when the fluoride ion concentration is reduced to below 10 mg/dm³ according to the Chinese industrial wastewater discharge standard. To reduce the harm to the water environment, it is usually required to carry out stricter emission standards, even below 1.5 mg/dm³ according to the Chinese regional standard DB 32/4440-2022.

<sup>&</sup>lt;sup>1</sup>School of Energy and Environment, Anhui University of Technology, Ma'anshan, China, corresponding author G. Sheng, email address: shenggh@ahut.edu.cn

Many removal methods of fluoride are used, such as precipitation, ion exchange, electrochemistry, membrane separation, adsorption [2], etc. Adsorption and precipitation methods are widely used because of their high removal rate, simple operation, and low cost. The precipitation method is often the first choice for treating high-concentration fluoride-containing wastewater [2]. Al, Ca, Fe, and other metal elements have a high affinity for fluoride ions, especially Al and Ca compounds are widely used to remove fluoride by precipitation [2]. For example, CaSO<sub>4</sub>·2H<sub>2</sub>O nanorods are used to treat high--concentration fluoride-containing wastewater. The fluoride removal process is dominated by precipitation, and the removal rate reaches over 95%, but the fluoride concentration in the effluent is still more than 10 mg/dm<sup>3</sup> [3]. Porous alumina hollow spheres prepared by hydrothermal and calcination treatment can remove over 95% of fluorides in a wide pH range, but it is only suitable for low-concentration fluoride-containing wastewater [4]. The fluoride removal efficiency can be further enhanced by compounding metal oxides, CaO·2Al<sub>2</sub>O<sub>3</sub> (CA<sub>2</sub>), synthesized by the calcination of CaO and Al<sub>2</sub>O<sub>3</sub> reduces the fluoride ion concentration to below 1.5 mg/dm<sup>3</sup>. However, it is not suitable for the treatment of high-concentration fluoride-containing wastewater [5]. Composite materials prepared by in-situ doping CaO·Al<sub>2</sub>O<sub>3</sub> (CA) into the diatomaceous earth skeleton increase the unit adsorption capacity to 18.22 mg/g as Ca<sup>2+</sup> ions are released during the fluoride removal process. But it is difficult to meet the requirements of high-concentration fluoride-containing wastewater treatment [6].

Cement-based materials, such as Portland cement and aluminate cement, etc. have the feasibility of fluoride removal because of high content of calcium and aluminum [7]. The hydrated Portland cement particle filter reduces the fluoride concentration from 407 mg/dm³ to less than 1 mg/dm³ owing to chemical precipitation and adsorption of calcium, and removes other anionic pollutants simultaneously [8]. The aluminate cement (calcium) containing CA, CA₂, and 12CaO·7Al₂O₃ (C₁₂A₁) has a good removal ability for low-concentration fluoride-containing wastewater [9], and further modification by calcination improves its fluoride removal performance, but the fluoride concentration after treatment is still over 10 mg/dm³ [10]. The sulphoaluminate cement modified by the hydrochloric acid increases the specific surface area and activity, but it is still difficult to remove the high concentration (> 100 mg/dm³) fluoride-containing wastewater to below 10 mg/dm³ [11]. The treatment of high-concentration fluoride-containing wastewater to a lower concentration, especially below 1 mg/dm³, is still very difficult. In this study, a novel two-step treatment process of high-concentration fluoride-containing wastewater by the modified CAC was investigated.

## 2. MATERIALS AND METHODS

Raw materials. CAC was purchased from Zhengzhou Sijihuo Refractory Co., Ltd. Its chemical composition (shown in Table 1) was mainly Al<sub>2</sub>O<sub>3</sub> and CaO, and a small amount of Na<sub>2</sub>O, SiO<sub>2</sub>, Mg<sub>2</sub>O, Fe<sub>2</sub>O<sub>3</sub>, and K<sub>2</sub>O.

Table 1
Chemical composition of the CAC

Component	Al <sub>2</sub> O <sub>3</sub>	CaO	Na <sub>2</sub> O	SiO <sub>2</sub>	MgO	Fe <sub>2</sub> O <sub>3</sub>	K <sub>2</sub> O
Content, %	70.97	26.63	0.706	0.563	0.225	0.207	0.021

All chemical reagents used were obtained from the Sinopharm Group Chemical Reagent Co., Ltd., except for HNO<sub>3</sub> from Dongfang Chemical Reagent Co., Ltd. All chemicals were analytical grade.

Preparation of modified CAC. The CAC and distilled water were thoroughly mixed at a 1:1 ratio (Fig. 1), then the mixture was hydrated in a sealed plastic bag at 25 °C for 3 days. The hydrated CAC sample was simply rinsed with distilled water and crushed, and then calcined in a furnace at 400~800 °C for 6 h. The calcined CAC was naturally cooled to room temperature in the furnace, and then ground into powder (< 0.1 mm) for fluoride adsorption. And part of them were ground using an agate mortar for XRD determination. The samples calcined at 400, 600, and 800 °C were designated as CAC-4, CAC-6 and CAC-8, respectively.

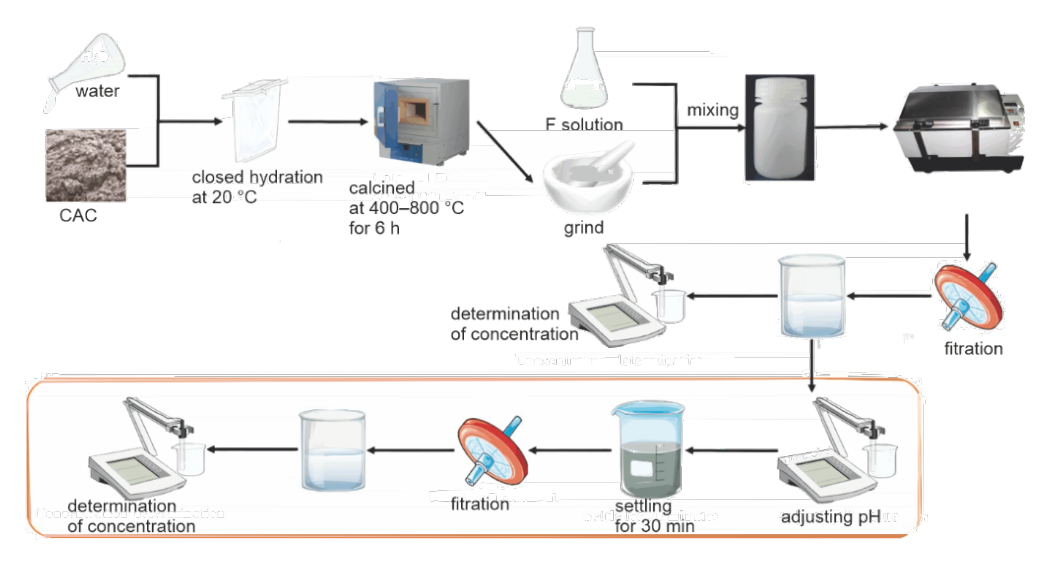


Fig. 1. Process of CAC modification and fluoride removal

Defluoridation test. 50 cm³ of fluoride-containing solution, prepared by analytical grade sodium fluoride reagent, with modified CAC was added to a 125 cm³ PTFE bottle, then put it into a water bath oscillator. At the set time, the supernatant was sucked and passed through a 0.45  $\mu$ m filter membrane for the determination of F⁻. The pH of the solution was adjusted with 0.1 mol/dm³ HNO₃ and 0.1 mol/dm³ NaOH solutions, and the ionic strength was adjusted with NaNO₃. The CO₃² , PO₃⁴ , NO₃ and SO₂⁴ anions in water

were simulated by adding NaCO<sub>3</sub>, NaH<sub>2</sub>PO<sub>4</sub>·2H<sub>2</sub>O, NaNO<sub>3</sub> and Na<sub>2</sub>SO<sub>4</sub>. The supernatant after the water bath oscillation reaction with modified CAC was taken to another beaker for the deep defluoridation, and the pH of the supernatant was adjusted with HCl and maintained for 30 min. After the reaction, the supernatant was filtered through a 0.45 μm filter membrane for the second determination of F<sup>-</sup>.

The fluoride removal rate  $\eta$ , % is given by

$$\eta = \frac{C_0 - C_e}{C_0} \times 100\% \tag{1}$$

where  $C_0$ ,  $C_e$ , mg/dm<sup>3</sup>, are the initial and final F<sup>-</sup> concentrations.

The adsorption capacity  $Q_e$ , mg/g, is

$$Q_e = \frac{C_0 - C_e}{m} \times V \tag{2}$$

where  $Q_e$ , mg/g, is the equilibrium adsorption capacity according to the adsorption test, V, dm<sup>3</sup>, is the volume of fluoride solution, m, g, is the mass of the added adsorbent.

Material analysis. The chemical compositions of the samples were determined by an X-ray fluorescence (XRF) method with an ARLAdvant'X Intellipower™3600 X-ray fluorescence spectrometer of Thermo Fisher Scientific. The X-ray diffraction spectrum (XRD) was determined using a Bruker D8 ADVANCE X-ray diffractometer, with the scanning range of 5–80 deg and the scanning speed of 5 deg/min. Field emission scanning electron microscopy (FE-SEM) was performed using a NANO SEM430 (FEI). Fourier transform infrared (FT-IR) spectra were recorded using a Nicolet 6700 FT-IR spectrometer (Thermo Nicolet Corporation) with a scanning range of 400–4000 cm⁻¹, a resolution of 1 cm⁻¹, and a continuous scanning mode.

The fluoride concentration was determined by the fluoride ion electrode method according to the Chinese standard *Determination of Fluoride in Water Quality (GB 7484-87)*. The calcium and aluminum ion concentrations were determined by the EDTA titration method according to the Chinese standard *Chemical Analysis Methods of Aluminate Cement*" (GB /T 205-2008).

Adsorption isotherm. Two-parameter isotherm models, Langmuir (Eq. (3)) [12] and Freundlich (Eq. (4)) [13], were used to describe the isothermal adsorption process.

$$\frac{C_e}{Q_e} = \frac{1}{K_L Q_m} + \frac{C_e}{Q_m} \tag{3}$$

$$\ln Q_e = \ln K_F + \frac{1}{n} \ln C_e \tag{4}$$

where:  $Q_m$ , mg/g, is the theoretical saturated adsorption capacity fitted by the Langmuir model,  $K_L$ , dm<sup>3</sup>/g, the adsorption equilibrium constant (or the adsorption coefficient),  $K_F$ , dm<sup>3</sup>/g, the Freundlich adsorption equilibrium constant, n is the adsorption intensity reflecting surface heterogeneity.

## 3. RESULTS AND DISCUSSION

#### 3.1. MINERAL CHANGES DURING HYDRATION AND CALCINATION

The early hydration products of CAC were mainly metastable  $CaO \cdot Al_2O_3 \cdot 10H_2O$  (CAH<sub>10</sub>) and  $2CaO \cdot Al_2O_3 \cdot 8H_2O$  (C<sub>2</sub>AH<sub>8</sub>), which gradually transformed into stable 3CaO  $\cdot Al_2O_3 \cdot 6H_2O$  (C<sub>3</sub>AH<sub>6</sub>) [14]. C<sub>3</sub>AH<sub>6</sub> was the main hydration product at 3 days (Fig. 2).

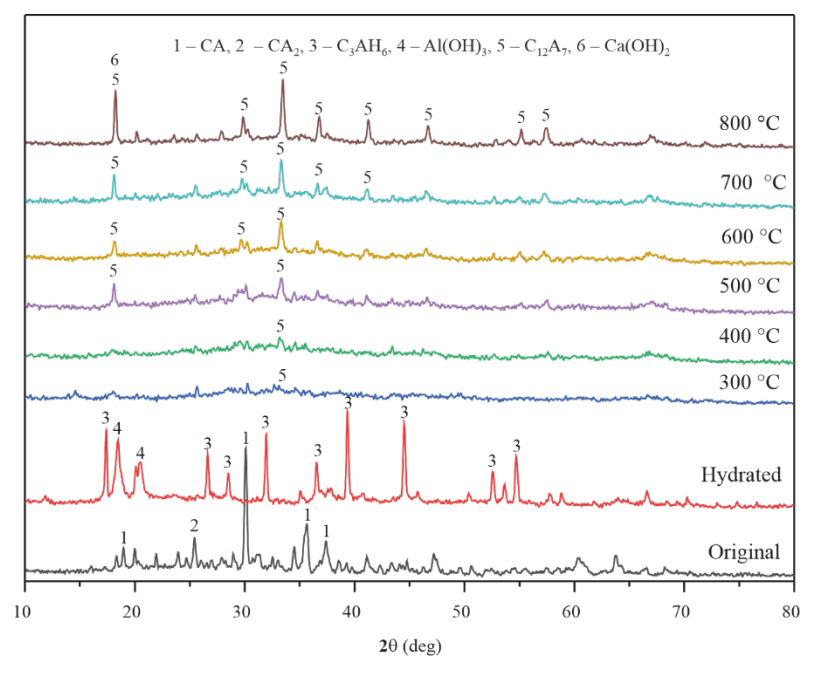


Fig. 2. XRD patterns of CAC after hydration and calcination

The hydration reaction of CAC is given in Eqs. (5) and (6) [15]:

$$3CA + 21H_2O \rightarrow CAH_{10} + C_2H_8 + Al(OH)_3$$
 (5)

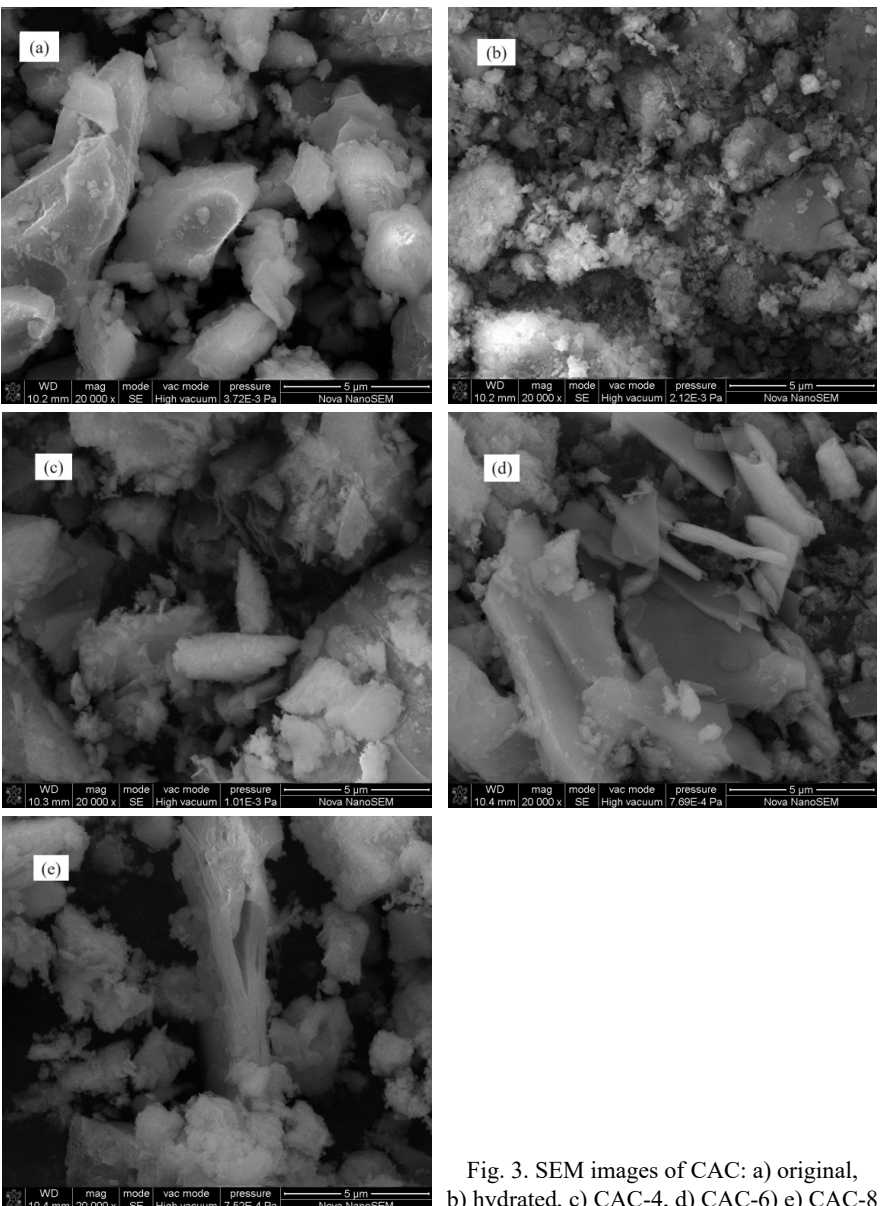
$$CAH_{10} + C_2AH_8 \rightarrow C_3AH_6 + Al(OH)_3 + 9H_2O$$
 (6)

C<sub>3</sub>AH<sub>6</sub> dehydrated and decomposed after calcination at 300 °C; the characteristic diffraction peaks of C<sub>3</sub>AH<sub>6</sub> disappeared, and the characteristic peaks of CA appeared.

88 G. SHENG et al.

When the calcination temperature increased to 400 °C, C<sub>12</sub>A<sub>7</sub> appeared, and its diffraction intensities increased with the increase of the calcination temperature, which had a better affinity for fluoride than C<sub>3</sub>AH<sub>6</sub> [10]. The decomposition reaction during calcination at a high temperature is given by [15]:

$$7C_3AH_6 \rightarrow C_{12}A_7 + 9CaO + 42H_2O$$
 (7)



b) hydrated, c) CAC-4, d) CAC-6) e) CAC-8

Raw CAC consisted mainly of irregular granular particles with a smooth surface (Fig. 3). After hydration, the particle surface became uneven, and many needles and floccules of hydration product  $C_3AH_6$  grew on the surface of the CAC particles. After calcination at 400 °C, flocs and needles gradually disappeared due to the dehydration of  $C_3AH_6$  and the appearance of flaky  $C_{12}A_7$ . With the calcination temperature increased to 600 °C and 800 °C, the sheets grew more, which indicated that all  $C_3AH_6$  transformed to  $C_{12}A_7$ .

### 3.2. FLUORIDE REMOVAL

Fluoride anions removal by modified CAC. As shown in Fig. 4a, the hydration treatment of CAC increased the removal rate of fluoride ions from 59.10 to 82.32%, and the removal rate furtherly improved to over 95% after calcination. This was because the main minerals in CAC were CA and 2CaO·SiO<sub>2</sub> (C<sub>2</sub>S), which could not be completely hydrated within 1 hour, while the main mineral in fully hydrated CAC was C<sub>3</sub>AH<sub>6</sub>, and Al(OH)<sub>3</sub> generated during the hydration process. Both showed good affinity for F<sup>-</sup>, improving its removal efficiency. After calcination, the original C<sub>3</sub>AH<sub>6</sub> transformed into C<sub>12</sub>A<sub>7</sub> and CaO with a stronger affinity for F<sup>-</sup>, while Al(OH)<sub>3</sub> transformed into Al<sub>2</sub>O<sub>3</sub>. During the process of fluoride removal, the generated CaO could also undergo chemical precipitation with F<sup>-</sup>, which finally showed a high fluoride removal rate.

Figure 4b showed that the rate of fluoride removal by CAC-6 was very high, and exceeded 95% after 5 min, and then slowly increased until the reaction equilibrium after 1 h.  $Ca^{2+}$  concentration in the solution rapidly increased to a high value of about 303 mg/dm<sup>3</sup> due to the quick hydration of  $C_{12}A_7$ , and reacted with  $F^-$  to form  $CaF_2$  sediment. At the same time, the new generation of  $Al(OH)_3$  had good adsorption ability of  $F^-$ . Hydration product  $C_3AH_6$  was also a better adsorbent for the  $F^-$ [16]. The hydration reactions of CAC-6 were as follows

$$C_{12}A_7 + 15H_2O \rightarrow 4C_3AH_6 + 6Al(OH)_3$$
 (8)

$$C_2S + H_2O \rightarrow Ca(OH)_2 + CSH$$
 (9)

As shown in Fig. 4c, the increase of initial pH from 2 to 3 improved the F<sup>-</sup> removal rate, and the removal rate of fluoride ions by CAC-6 remained at about 99% when the initial pH of fluoride ion solution was in the range of 3 to 12. The hydration reaction of C<sub>12</sub>A<sub>7</sub> occurred immediately after CAC-6 was added to water. Ca<sup>2+</sup> ions quickly released into the solution and their concentration increased to 303 mg/dm<sup>3</sup> (shown in Fig. 6). The final pH of the solution quickly increased to 5.5 after CAC-6 adding, and then gradually increased to 12, and maintained at about 11.5 with the initial pH from 4 to 11, which was conducive to the formation of CaF<sub>2</sub> precipitation reaction by Ca<sup>2+</sup> and F<sup>-</sup>. When the initial pH was 2, the solution after the reaction was still acidic, pH ca. 5.5, because CaO generated by hydration could not consume H<sup>+</sup> ions in the solution. As a result, F<sup>-</sup> existed

as HF under acidic conditions, which was unfavorable for fluoride removal by Ca<sup>2+</sup> [17]. The solubility of CaF<sub>2</sub>, increasing under acidic conditions, also resulted in a decrease in the fluoride removal rate [18]. When the initial pH was 12, the fluoride removal rate decreased. The pH<sub>zpc</sub> of CAC-6 was 9.93 [10], so the surface of CAC-6 deprotonated and the electrostatic repulsion was generated between fluoride ions and the CAC-6 particle surfaces; meanwhile, the competition adsorption between OH<sup>-</sup> and F<sup>-</sup> reduced the fluoride removal rate [19]. And Ca ion in the solution mainly existed in the form of Ca(OH)<sup>+</sup> and Ca(OH)<sub>2</sub>(aq) [20], which were not conducive to the generation of CaF<sub>2</sub> precipitation. As a result, the fluoride removal rate decreased at pH of 12.

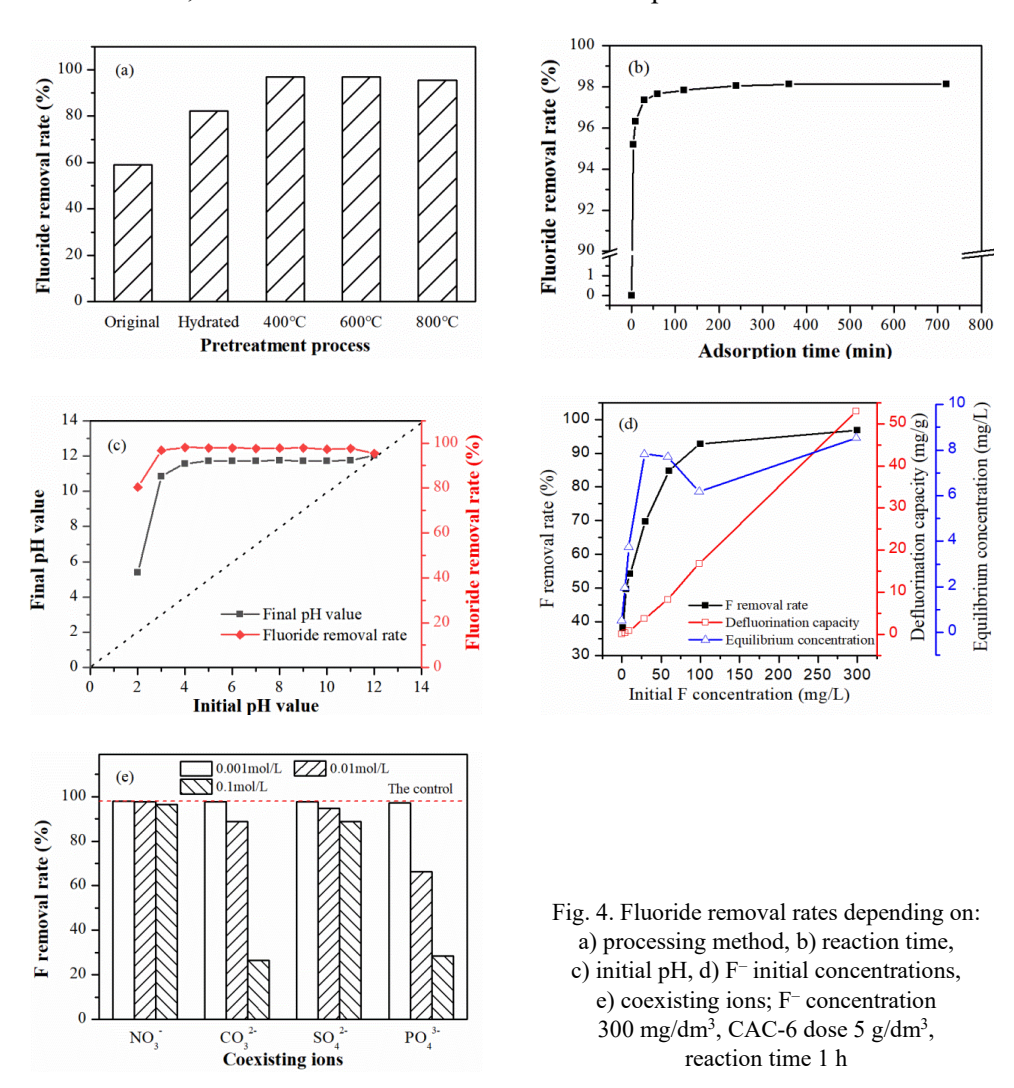


Figure 4d shows that the fluoride removal rate by CAC-6 was positively correlated with the initial concentration, which differed from typical adsorbents. The increase in fluoride ion concentration enhanced the hydration reaction rate of C<sub>12</sub>A<sub>7</sub>, which released more Ca<sup>2+</sup> and amorphous Al(OH)<sub>3</sub> and improved the precipitation reaction of CaF<sub>2</sub>. The Ca<sup>2+</sup> concentration was 303 mg/dm<sup>3</sup>, according to the solubility product principle, a higher F<sup>-</sup> concentration was beneficial to the CaF<sub>2</sub> precipitation reaction. The final F<sup>-</sup> concentration by CAC-6 removal increased with the increase in the initial F<sup>-</sup> concentration. It reached about 7–8 mg/dm<sup>3</sup> and remained almost unchanged when the initial F<sup>-</sup> concentration increased to more than 30 mg/dm<sup>3</sup>. It was close to the theoretically calculated concentrations of F<sup>-</sup> precipitation by lime precipitation [21].

Figure 4e shows that the  $CO_3^{2-}$ ,  $SO_4^{2-}$ , and  $PO_4^{3-}$  anions inhibited the removal of fluoride by CAC-6, and higher anion concentration resulted in a stronger inhibitory effect, while  $NO_3^-$  hardly affected the fluoride removal. The inhibiting order was expressed as  $PO_4^{3-} > CO_3^{2-} > SO_4^{2-} > NO_3^-$ , which agreed with the charge/radius (Z/r) order,  $PO_4^{3-} > CO_3^{2-} > SO_4^{2-} > F^- > NO_3^-$ . The ion ranked ahead of  $F^-$  in the Z/r order had a stronger affinity with  $Ca^{2+}$  than  $F^-$ . As a result,  $PO_4^{3-}$ ,  $CO_3^{2-}$ , and  $SO_4^{2-}$  ions inhibited the fluoride removal [22], especially  $PO_4^{3-}$  and  $CO_3^{2-}$  ions in 0.1 mol/dm³ solutions had a great effect on the fluoride removal. The rank of  $NO_3^-$  was behind  $F^-$ , so the adsorption of fluoride was not affected by  $NO_3^-$ , even at higher concentrations.

Table 2 The solubility product constants  $K_{\rm sp}$  at 25 °C

Compound	$K_{\rm sp}$ at 25 ° C [23]	Ion-concentration product, $I_{\text{sp}}$	Saturation inday = I V
Compound	Asp at 23 C[23]	Ton-concentration product, Isp	Saturation index – $I_{sp}/K_{sp}$
Ca <sub>3</sub> (PO <sub>4</sub> ) <sub>2</sub>	2.07×10 <sup>-33</sup>	$4.32 \times 10^{-11}$	$2.09 \times 10^{22}$
CaCO <sub>3</sub>	3.36×10 <sup>-9</sup>	7.56×10 <sup>-5</sup>	22500
CaF <sub>2</sub>	3.45×10 <sup>-11</sup>	7.56×10 <sup>-7</sup>	21913
CaSO <sub>4</sub>	3.14×10 <sup>-5</sup>	756×10 <sup>-5</sup>	2.4
Ca(NO <sub>3</sub> ) <sub>2</sub>	soluble		_

 $\ll$ 

Table 2 shows the solubility product constants of the  $PO_4^{3-}$ ,  $CO_3^{2-}$ ,  $SO_4^{2-}$ ,  $NO_3^{-}$  with  $Ca^{2+}$  ions. When the concentrations of cations and anions were equal, the saturation index followed the order  $Ca(NO_3)_2 < CaSO_4 < CaF_2 < CaCO_3 \ll Ca_3(PO_4)_2$ . This indicated that  $Ca_3(PO_4)_2$  and  $CaCO_3$  were more likely to precipitate than  $CaF_2$ , especially  $Ca_3(PO_4)_2$ , while  $CaSO_4$  did not precipitate. As a result,  $PO_4^{3-}$  and  $CO_3^{2-}$  decreased the  $F^-$  removal rate by CAC-6, because those anions preferentially reacted with  $Ca^{2+}$  in the solution and covered the surface of CAC-6 particles or consumed the  $Ca^{2+}$ .

Fluoride anion removal by pH modification. After the fluoride ion solution was treated by CAC-6, the pH of the filtrate was about 11.5, and the F<sup>-</sup> ion concentration was 11.30 mg/dm<sup>3</sup>. After the pH was diminished to under 10, the solution became turbid, and the fluoride removal rate increased (Fig. 5). When the pH was decreased from 8 to 5, the fluoride removal rate increased to more than 95%, and the fluoride concentration decreased below 0.5 mg/dm<sup>3</sup>. If the pH was modified to under 5, the solution gradually became clear, and the fluoride removal rate decreased. Therefore, the fluoride ions were deeply removed by modifying the pH of the solution after CAC-6 treatment.

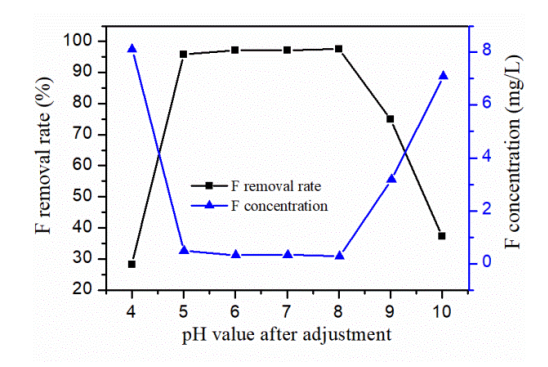


Fig. 5. Effect of pH on deep fluoride removal

### 3.3. CALCIUM ION AND ALUMINUM ION LEACHING

Calcium ion leaching. Figure 6 shows that the leaching concentration of Ca<sup>2+</sup> of CAC in distilled water was 207.77 mg/dm<sup>3</sup> and reduced to 118.32 mg/dm<sup>3</sup> after hydration treatment, and then increased after calcination treatment. When the calcination temperature reached 400, 600, and 800 °C, the concentration of Ca<sup>2+</sup> increased to 261.88, 303.00, and 431.42 mg/dm<sup>3</sup>, respectively.

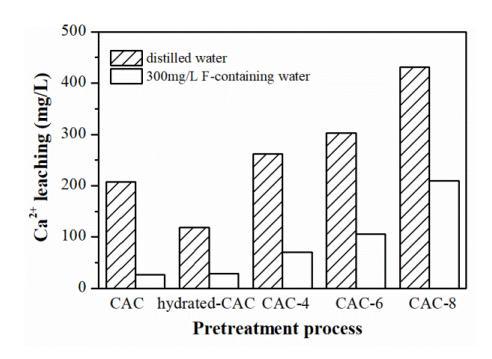


Fig. 6. Ca<sup>2+</sup> leaching from CAC; CAC dose 5 g/dm<sup>3</sup>, reaction time 1 h

The main minerals of untreated CAC were CA and C<sub>2</sub>S, which reacted with water to generate Ca(OH)<sub>2</sub>, resulting in the release of Ca<sup>2+</sup> into water. After hydration, CA transformed to low solubility C<sub>3</sub>AH<sub>6</sub>, and C<sub>2</sub>S transformed to hydrated calcium silicate,

which reduced the dissolution of  $Ca^{2+}$ . The  $C_3AH_6$  decomposed to  $C_{12}A_7$  and lime (CaO) after calcination at high temperature [24]. The hydration of  $C_{12}A_7$  was faster than that of  $C_3A$ . As a result, the calcined hydrated CAC released more  $Ca^{2+}$  in a short time after being added to water. According to the chemical reaction, 7 mol  $C_3AH_6$  decomposition produced 9 mol of CaO and 1 mol of  $C_{12}A_7$  (Eq. (7)), and a higher temperature was beneficial to the decomposition of  $C_3AH_6$  and generated more CaO and  $C_{12}A_7$ , so the concentration of  $Ca^{2+}$  increased at a higher temperature. The concentration of  $Ca^{2+}$  in the fluoride solution was lower than that in distilled water (Fig. 6) because  $F^-$  ions reacted with  $Ca^{2+}$  and generated  $CaF_2$ , which partly covered the surface of CAC-6 particles and decreased their dissolution.  $Ca^{2+}$  leaching of CAC-6 played an important role in fluoride removal by CAC-6. The  $CaF_2$  ion concentration product from the  $Ca^{2+}$  leaching of CAC with different treatment methods was calculated at a fluoride ion concentration of 303 mg/dm³. Concerning the results shown in Table 3, it is evident that the  $I_{sp, cal}$  is greater than the  $I_{sp, cal}$  is

Table 3

Calculation results of ion product

Material	Calcium ion leaching concentration (mol/dm <sup>3</sup> )	$I_{\text{sp cal}} = [\text{Ca}^{2+}] \times [\text{F}^{-}]^2$
Original	5.18×10 <sup>-3</sup>	8.17×10 <sup>-5</sup>
Hydrated	2.95×10 <sup>-3</sup>	4.66×10 <sup>-5</sup>
CAC-4	6.53×10 <sup>-3</sup>	1.03×10 <sup>-4</sup>
CAC-6	7.56×10 <sup>-3</sup>	1.19×10 <sup>-4</sup>
CAC-8	10.76×10 <sup>-3</sup>	1.70×10 <sup>-4</sup>

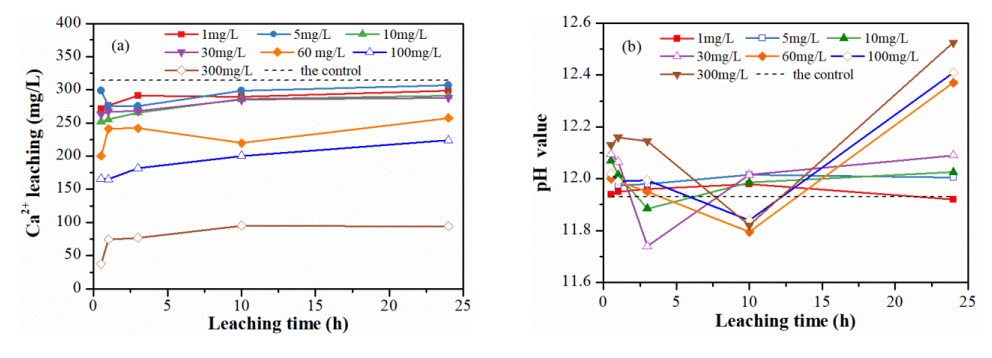


Fig. 7. Time profiles of Ca<sup>2+</sup> concentration (a) and pH (b) in F<sup>-</sup> solutions; CAC-6 dose 5 g/dm<sup>3</sup>

The Ca<sup>2+</sup> leaching concentration of CAC-6 in the solution containing fluoride decreased with the increase of fluoride concentration, while pH increased with the increase of fluoride concentration (Fig. 7). The leaching concentration reached equilibrium in about 3 h, which was similar to the equilibrium time of fluoride removal. The chemical

precipitation of  $CaF_2$  was more likely to occur with the increase of fluoride ion concentration. The theoretical consumption of  $Ca^{2+}$  was much larger than the actual reduction when the fluoride ion concentration in the solution was higher than  $30 \text{ mg/dm}^3$ . It meant that the material increased the release of  $Ca^{2+}$  in the actual fluoride removal process, and the release of  $Ca^{2+}$  increased the pH of the solution.

Aluminum leaching. The concentration of dissolved  $Al^{3+}$  of CAC-6 in distilled water and 300 mg/dm<sup>3</sup> fluoride ion solution was 149.63 mg/dm<sup>3</sup> and 375 mg/dm<sup>3</sup>, respectively (Fig. 8). The concentration of  $Al^{3+}$  increased significantly in  $F^-$  solution, because  $CaF_2$  precipitates with  $Ca^{2+}$  and  $F^-$ , which promoted the hydration of  $C_{12}A_7$  and released more  $Al^{3+}$  into the solution.

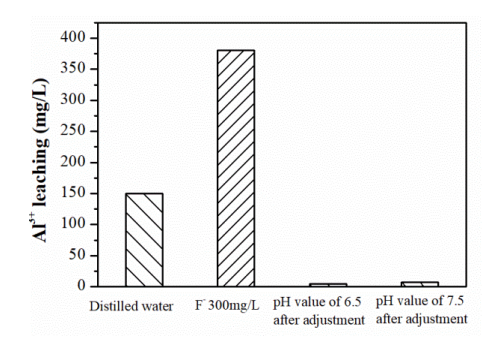


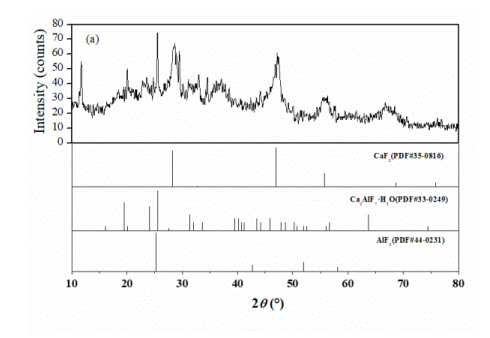
Fig. 8. Al<sup>3+</sup> leaching in various solutions; CAC-6 doses 5 g/dm<sup>3</sup>)

When the pH of the filtrate was decreased to 7.5 and 6.5, the solution became turbid, and the residual concentration of aluminum ions in the supernatant sharply decreased to 7.43 and 4.65 mg/dm³, respectively. Under alkaline conditions, Al existed in the form of Al(OH)<sub>4</sub> ions [25], and transformed to insoluble Al(OH)<sub>3</sub> when pH decreased. Therefore, the concentration of Al in the solution was reduced [26]. The newly generated Al(OH)<sub>3</sub> was a good adsorbent for F<sup>-</sup> due to the electrostatic interaction and ion exchange [27]. As a result, the concentration of F<sup>-</sup> sharply decreased. When the pH was decreased to less than 5, Al mainly existed in the form of Al<sup>3+</sup> ions, which was unbeneficial to F<sup>-</sup> removal. A little Al existed in the form of Al(OH)<sub>4</sub> at pH 7, resulting in the residual concentration of Al<sup>3+</sup> in the effluent higher than 0.2 mg/dm³.

## 3.4. MECHANISM ANALYSIS

As seen in Fig. 9a, the  $C_{12}A_7$  characteristic peaks of CAC-6 after adsorption disappeared, while new diffraction peaks at  $2\theta$  of  $28.266^{\circ}$ ,  $47.004^{\circ}$  and  $55.763^{\circ}$  appeared, which belonged to  $CaF_2$  (PDF#35-0816). The diffraction peak at  $25.229^{\circ}$  belonged to AlF<sub>3</sub> (PDF#44-0231), and the diffraction peaks at  $19.450^{\circ}$ ,  $24.098^{\circ}$ ,  $25.576^{\circ}$ ,  $31.339^{\circ}$  and  $63.685^{\circ}$  belonged to  $Ca_2AlF_7 \cdot H_2O$  (PDF#33-0249). The appearance of  $CaF_2$ ,  $AlF_3$ 

and  $Ca_2AlF_7 \cdot H_2O$  after fluoride removal indicated that CAC-6 successfully captured fluoride ions in the solution during the treatment. In addition, the appearance of  $CaF_2$  proved the chemical precipitation of  $Ca^{2+}$  and  $F^-$ , and the appearance of  $AlF_3$  and  $Ca_2AlF_7 \cdot H_2O$  after the reaction indicated that there was also chemical adsorption in the process of fluoride removal.



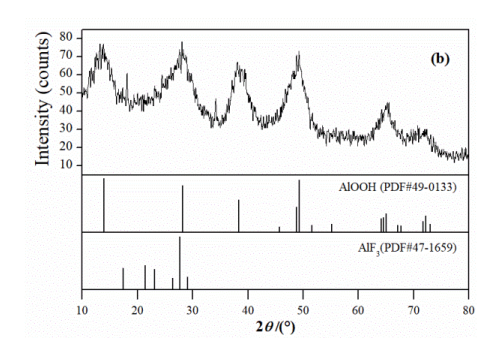


Fig. 9. XRD spectra of samples after adsorption (a) and pH modification (b)

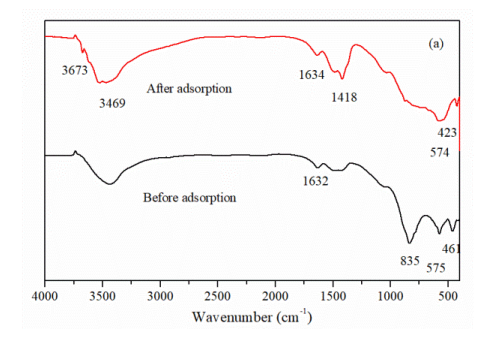
 $Al_2O_3$  was the main component of the sediment during pH modification, and a few  $F^-$  ions existed (Table 4). The existence of  $Al_2O_3$  was due to the hydration of  $C_{12}A_7$  and the precipitation of  $Al_3^{3+}$  by pH modification. The diffraction peaks at  $2\theta$  of  $14.001^\circ$ ,  $28.199^\circ$ ,  $38.287^\circ$ ,  $49.325^\circ$ ,  $65.031^\circ$  and  $72.222^\circ$  (Fig. 9b) belonged to AlOOH (PDF#49-0133). And the diffraction peak at  $2\theta$  of  $27.745^\circ$  was consistent with the XRD standard spectrum of  $AlF_3$  (PDF#47-1659), which indicated that fluoride ion was adsorbed and removed by flocculation and precipitation. It was the reason for  $F^-$  removal during the pH modification process.

Table 4
Chemical compositions of sediment during pH modification process

Chemical component	Al <sub>2</sub> O <sub>3</sub>	F	CaO	MgO	SiO <sub>2</sub>	Na <sub>2</sub> O
Content, %	97.80	1.55	0.308	0.110	0.081	0.026

The FT-IR spectra of CAC-6 (Fig. 10a) showed that the vibration band of CAC-6 at 3434 cm<sup>-1</sup> was assigned to the expansion and contraction of hydroxyl groups after water absorption, and 1the band at 632 cm<sup>-1</sup> was assigned to the vibration peak formed by the bending of hydroxyl groups after water absorption [28]. The band at 1418 cm<sup>-1</sup> was assigned to an asymmetric expansion and contraction vibration of CO<sub>2</sub><sup>2-</sup>, which was due to the introduction of CO<sub>2</sub> in the air into the solution during the defluoridation reaction [29]. The band at 1033 cm<sup>-1</sup> belonged to the aluminum functional group, and the absorption bands at 825, 575, and 461 cm<sup>-1</sup> belonged to the metal bond (M–O), which was assigned as Al–O and Ca–O according to chemical composition [30]. After

fluoride removal by CAC-6, the absorption band at 825 cm<sup>-1</sup> was weaker, indicating that Al–O or Ca–O played a role in the reaction process [31].



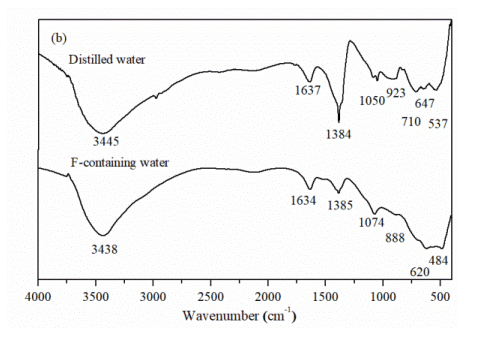


Fig. 10. FT-IR spectra of CAC-6 (a) and deep defluoridation precipitates (b)

Figure 10b showed that the flocculated sediment in distilled water displays vibration peaks formed by the stretching and bending of hydroxyl groups at 3445 and 1637cm<sup>-1</sup>, the vibration peaks formed by the asymmetric and symmetric bending of AlOOH at 1384 and 1050cm<sup>-1</sup>, and the vibration peaks at 923, 710, 647, and 537 cm<sup>-1</sup> [32]. In contrast, the absorption peaks of the flocculated sediments of the second-stage defluoridation all shifted, indicating the formation of Al–F, while the absorption peak was weaker at 1385 cm<sup>-1</sup>, indicating that the Al–OH bond was broken. At the same time, during the flocculation and precipitation of Al–OH, the hydroxyl groups in it would exchange ions with F<sup>-</sup> in the solution, thus realizing the deep removal of fluoride ions [31].

## 3.5. ISOTHERMAL ADSORPTION FITTING

The results presented in Fig. 11 and Table 5 show that if the initial fluoride concentration was not higher than 30 mg/dm³, the fitting coefficients ( $R^2$ ) of Langmuir and Freundlich models were 0.865 and 0.993, respectively. Thus, the adsorption behavior of CAC-6 was better described by the Freundlich model. It meant that it was a multilayer adsorption of fluoride ions at lower concentrations [33]. As the initial concentration of fluoride ions continued to increase (> 30 mg/dm³), the experimental data deviated from the fitting curves of the two models, indicating that the defluoridation mechanism of CAC-600 at this time was not only surface adsorption. In addition, with the increase of the initial concentration of fluoride, the equilibrium fluoride concentration decreased, and tended to be about 8 mg/dm³ when the initial concentration was over 100 mg/dm³. This was because the chemical precipitation between Ca²+ and F⁻ generally occurred at high concentration, and fluoride ions could only be reduced to a certain level (about 8 mg/dm³). Therefore, at low initial concentration, the fluoride removal of CAC-6 was mainly dependent on adsorption, and the equilibrium fluoride concentration increased with the initial fluoride concentration. When the fluoride concentration was

high, the adsorption gradually reached saturation, but the fluoride concentration in the system was still high at this time, and the chemical precipitation of Ca<sup>2+</sup> and F<sup>-</sup> occurred more easily.

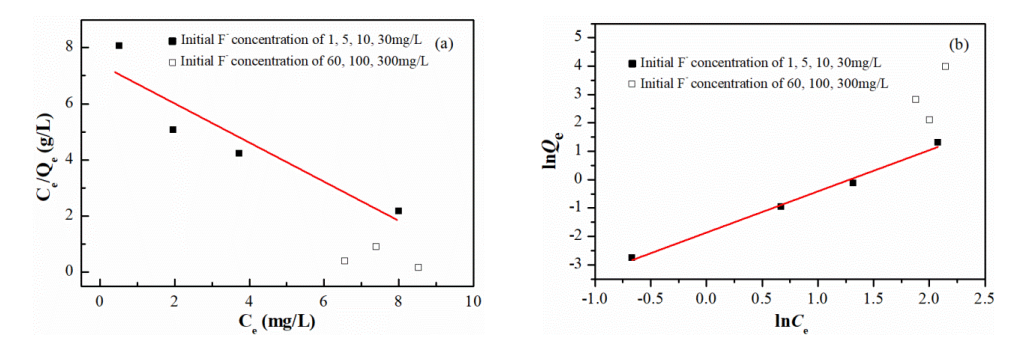


Fig. 11. Fitting of isothermal adsorption Langmuir (a) and Freundlich (b) models

Table 5

Isotherm model parameters at 25 °C

Langmuir isotherm Freundlich isotherm

Langmuir isotherm			Freundlich isotherm			
$Q_n$ [mg/	' [g]	$K_{\rm L}$ [dm <sup>3</sup> /g]	$R^2$	$K_{\rm F}$ [dm <sup>3</sup> /g]	n	$R^2$
1.42	29	0.095	0.865	0.155	1.4514	0.993

During the massive precipitation of CaF<sub>2</sub>, the leached Ca<sup>2+</sup> ions were consumed continuously, which further promoted the release of Ca<sup>2+</sup> and Al<sup>3+</sup> in CAC-600 and enhanced the fluoride removal to a certain extent, so the equilibrium fluoride concentration appeared at the initial concentrations of 60 mg/dm<sup>3</sup> and 100 mg/dm<sup>3</sup>. However, with the continuous increase of the initial concentration, the enhancement of this part was not significant, and the equilibrium fluoride concentration began to increase. The equilibrium fluoride concentration was maintained at about 8 mg/dm<sup>3</sup> due to the sufficient concentration of Ca<sup>2+</sup>. The fitting results of the two models further pointed out that there were two mechanisms of fluoride removal in CAC-6, namely surface adsorption and chemical precipitation, and the surface adsorption was more obvious at low concentrations, but the chemical precipitation gradually replaced it and dominated at high concentrations [34].

## 4. CONCLUSIONS

• The main component of CAC-6 is  $C_{12}A_7$ , which has excellent fluoride removal performance in a wide pH range. The removal rate increases with the increase of fluoride ion concentration, but it is inhibited by  $PO_4^{3-}$ ,  $CO_3^{2-}$  and  $SO_4^{2-}$ , and the fluoride

removal process is faster. Two-step treatment, adsorption and pH-value adjustment, can remove the fluoride from 300mg/dm<sup>3</sup> to less than 1 mg/dm<sup>3</sup>.

• The defluoridation process of CAC-6 depends on chemical precipitation, as well as some surface and electrostatic adsorption. The chemical precipitation plays an important role in high concentration, while the adsorption shows a main effect in low concentration. The defluoridation during the pH modification process mainly depends on the reaction of F<sup>-</sup> and AlOOH and the adsorption.

### ACKNOWLEDGMENT

The authors are grateful for financial support from the research Fund of the Engineering Research Center of Biofilm Water Purification and Utilization Technology of the Ministry of Education (BWPU2021 KF07, BWPU2021ZY02).

#### REFERENCES

- [1] GHOSH S., MALLOUM A., IGWEGBE C.A., IGHALO J.O., AHMADI S., DEHGHANI M.H., OTHMANI A., GÖKKUŞ Ö., MUBARAK N.M., New generation adsorbents for the removal of fluoride from water and wastewater: A review, J. Mol. Liq., 2022, 346, 118257. DOI: 10.1016/j.molliq.2021.118257.
- [2] SUN Y., ZHANG C., MA J., SUN W., SHAH J.K., Review of fluoride removal technology from wastewater environment, Desalin. Water Treat., 2023, 299 (7), 90–101. DOI: 10.5004/dwt.2023.29668.
- [3] SHAO S., MA B.Z., CHEN Y.Q., ZHANG W., WANG C., Behavior and mechanism of fluoride removal from aqueous solutions by using synthesized CaSO<sub>4</sub>·2H<sub>2</sub>O nanorods, Chem. Eng. J., 2021, 426 (11), 131364. DOI: 10.1016/j.cej.2021.131364.
- [4] ZHANG Y.X., JIA Y., Preparation of porous alumina hollow spheres as an adsorbent for fluoride removal from water with low aluminum residual, Ceram. Int., 2016, 42 (15), 17472–17481. DOI: 10.1016/j.ceramint.2016.08.052.
- [5] SAKHARE N., LUNGE S., RAYALU S., BAKARDJIVA S., SUBRT J., DEVOTTA S., LABHSETWAR N., Defluoridation of water using calcium aluminate material, Chem. Eng. J., 2012, 203 (9), 406–414. DOI: 10.1016 /j.cej.2012.07.065.
- [6] OLADOJA N.A., HELMREICH B., Calcium aluminate-diatomaceous earth composite as a reactive filter material for aqua defluoridation, J. Water Process Eng., 2016, 9 (2), 58–66. DOI: 10.1016/j.jwpe.2015.11.012.
- [7] KAGNE S., JAGTAP S., DHAWADE P., KAMBLE S.P., DEVOTTA S., RAYALU S.S., *Hydrated cement:* A promising adsorbent for the removal of fluoride from aqueous solution, J. Hazard. Mater., 2008, 154 (1–3), 88–95. DOI: 10.1016/j.jhazmat.2007.09.111.
- [8] PARK J.Y., BYUN H.J., CHOI W.H., KANG W.H., Cement paste column for simultaneous removal of fluoride, phosphate, and nitrate in acidic wastewater, Chemosphere, 2008, 70 (8), 1429–1437. DOI: 10.1016/j.chemosphere.2007.09.012.
- [9] AYOOB S., GUPTA A.K., BHAKAT P.B., BHAT V.T., Investigations on the kinetics and mechanisms of sorptive removal of fluoride from water using alumina cement granules, Chem. Eng. J., 2008, 140 (1–3), 6–14. DOI: 10.1016/j.cej.2007.08.029.
- [10] REN Y.X., QIAN Z., ZHAO C.L., CHENG P., YANG L., Behavior of fluoride adsorption onto thermally dehydrated aluminate cement granules, J. Build. Mater., 2020, 23 (2), 421–429. DOI: 10.1016/j.cej.2007.08.029.
- [11] XIE Y.H., HUANG J.Q., WANG H.Q., LV S.Y., JIANG F., PAN Z.C., LIU J., Simultaneous and efficient removal of fluoride and phosphate in phosphogypsum leachate by acid-modified sulfoaluminate cement, Chemosphere, 2022, 305 (10), 135422. DOI: 10.1016/j.chemosphere.2022.135422.

- [12] LANGMUIR I., The constitution and fundamental properties of solids and liquids, J. Am. Chem. Soc., 1916, 38 (11), 2221–2295. DOI: 10.1016/S0016-0032 (17)90938-X.
- [13] FREUNDLICH H.M., Over the adsorption in solution, J. Phys. Chem., 1906, 57, 385–470. DOI: 10.1515/zpch-1907-5723.
- [14] GOERGENS J., MANNINGER T., GOETZ-NEUNHOEFFER F., *In-situ XRD study of the temperature-dependent early hydration of calcium aluminate cement in a mix with calcite*, Cem. Concr. Res., 2020, 136 (10), 106160. DOI: 10.1016/j.cemconres.2020.106160.
- [15] KHALIQ W., KHAN H.A., High temperature material properties of calcium aluminate cement concrete, Constr. Build. Mater., 2015, 94 (2), 475–487. DOI: 10.1016/j.conbuildmat.2015.07.023.
- [16] Guo M.L., XIAO J., Zuo S.H., *Chloride binding capcacity of hydrated C<sub>3</sub>A pastes*, J. Build. Mater., 2019, 22 (3), 341–347. DOI: 10.3969/j.issn.1007-9629.2019.03.003.
- [17] CHEN N., DONG M.F., KONG H.X., ZHANG L., HE W.G., YIN T.P., CHEN C.M., ZHAO M.J., Selection test of agents for secondary treatment of photovoltaic wastewater and engineering application, China Water Wastewater, 2023, 39 (18), 100–106. DOI: 10.19853/j.zgjsps.1000-4602.2023.18.017.
- [18] SHAO S., MA B.Z., CHEN Y.Q., ZHANG W., WANG C., Behavior and mechanism of fluoride removal from aqueous solutions by using synthesized CaSO<sub>4</sub>·2H<sub>2</sub>O nanorods, Chem. Eng. J., 2021, 426 (11), 131364. DOI: 10.1016/j.cej.2021.131364.
- [19] SINGH S., CHAUDHARI S., Fluoride mitigation by co-precipitation in calcium phosphate systems: Effect of process parameters and presence of synthetic non-calcined hydroxyapatite, J. Water Proc. Eng., 2023, 53 (7), 103765. DOI: 10.1016/j.jwpe.2023.103765.
- [20] CUI B., JIN Y., YANG Z.K., Research on the treatment of high fluoride wastewater by calcium salt coagulation method, Ind. Water Treat., 2023, 43 (6), 150–155. DOI: 10.19965/j.cnki.iwt.2022-0724.
- [21] LI J.Y., YANG X., HUANG W.W., LUO B.F., CHEN Q., HUNAG Y.Q., Deep fluoride removal from fluoridated industrial wastewater based on two-stage enhanced chemical coagulation and precipitation method, Technol. Water Treat., 2024, 50 (2), 121–124. DOI: 10.16796/j.cnki.1000-3770.2024.02.022.
- [22] CHEN L., ZHANG K.S., HE J.Y., XU W.H., HUANG X.J., LIU J.H., Enhanced fluoride removal from water by sulfate-doped hydroxyapatite hierarchical hollow microspheres, Chem. Eng. J., 2016, 285 (2), 616–624. DOI: 10.1016/j.cej.2015.10.036.
- [23] HAYNES W.M., CRC Handbook of Chemistry and Physics, CRC Press, Boca Raton, 2016. DOI: 10.1205/cherd.br.0605.
- [24] WANG Y.L., LI X.C., ZHU B.Q., CHEN P.G., Microstructure evolution during the heating process and its effect on the elastic properties of CAC-bonded alumina castables, Ceram. Int., 2016, 42 (9), 11355–11362. DOI: 10.1016/j.ceramint.2016.04.058.
- [25] LUAN Z.K., The speciation and speciation stuty of aluminum in water, Environ. Chem., 1987, 6 (1), 46–56. DOI: 10.7524/j.issn.0254-6108.2023121001.
- [26] WANG M., MAO Y.H., CHEN C., BAI D., *Progress on the toxicity, morphology and control of aluminum salt hydrolysates in water treatment process*, Chem. Ind. Eng. Prog., 2023, 42 (S1), 479–488. DOI: 10.16085/j.issn.1000-6613.2023-1056.
- [27] WANG X., Xu H., WANG D., Mechanism of fluoride removal by AlCl<sub>3</sub> and Al13: The role of aluminum speciation, J. Hazard. Mater., 2020, 298 (11), 122987. DOI: 10.1016/j.jhazmat.2020.122987.
- [28] JIN H.Y., JI Z.J., YUAN J., LI J., LIU M., XU C.H., DONG J., HOU P., HOU S.E., Research on removal of fluoride in aqueous solution by alumina-modified expanded graphite composite, J. Alloys Compd., 2015, 620 (1), 361–367. DOI: 10.1016/j.jallcom.2014.09.143.
- [29] TAS A.C., Chemical preparation of the binary compounds in the calcia-alumina system by self-propagating combustion synthesis, J. Am. Ceram. Soc., 1998, 81 (11), 2853–2863. DOI: 10.1111/j.1151-2916.1998.tb02706.x.
- [30] AL-GHOUTI M.A., KHAN M., MALIK A., KHRAISHEH M., HIJAZI D.A., MOHAMED S.I., ALSOROUR S., ELTAYEB R.Y., AL-MAHMOUD F., ALAHMAD J.K., Development of novel nano-γ-Al<sub>2</sub>O<sub>3</sub> adsorbent from

- waste aluminum foil for the removal of boron and bromide from aqueous solution, J. Water Proc. Eng., 2022, 50 (12), 103312. DOI: 10.1016/j.jwpe.2022.103312.
- [31] SUJANA M.G., ANAND S., Iron and aluminium based mixed hydroxides: a novel sorbent for fluoride removal from aqueous solutions, Appl. Surf. Sci., 2010, 256 (23), 6956–6962. DOI: 10.1016/j.apsusc.2010.05.006.
- [32] Lv F.C., Li Z.L., Zou T., Li Y.B., Zhang W.G., Cao X.J., Chen Y., Preparation and characterization of γ-AlOOH/Fe<sub>3</sub>O<sub>4</sub> for the highly effective removal of Congo red from wastewater, J. Phys. Chem. Solids, 2023, 186 (3), 111830. DOI: 10.1016/j.jpcs.2023.111830.
- [33] YANG Y., KOH K.Y., LI R., ZHANG H.P., YAN Y., CHEN J.P., An innovative lanthanum carbonate grafted microfibrous composite for phosphate adsorption in wastewater, J. Hazard. Mater., 2020, 392 (6), 121952. DOI: 10.1016/j.jhazmat.2019.121952.
- [34] LI Z.X., ZHU Z., HUA C., ZHANG S., GUI W.J., HUANG L.D., YU F., PAN D.Q., Study on delimiting the dominance of the removal mechanisms of fluoride by calcite in open system, Environ. Sci. Technol., 2023, 46 (5), 1–9. DOI: 10.19672/j.cnki.1003-6504.1911.22.338.